International Journal of Mechanical and Electrical Engineering
ISSN: 3005-9615 (Print), ISSN: 3005-7132 (Online)
Volume 8, Number 8, Year 2026
DOI: https://doi.org/10.62051/ijmee.v8n8.04

Comparative Analysis of Mass Reduction in a Triangular Grooved Drill-Rod Body

Mengchao Duan *

School of Mechanical and Power Engineering, Henan Polytechnic University, Jiaozuo, Henan, 454003, China

* Corresponding Author: Mengchao Duan

ABSTRACT

Thirteen geometric configurations of a previously developed triangular grooved drill-rod body were compared to reduce the burden of manual handling, connection and disconnection. The body length and maximum outer diameter were fixed at 1000 and 89 mm, respectively, and the original end structures were retained. Each configuration had three helical grooves and three flat grooves of equal depth. Numerical result summaries under an axial tensile force of 190 kN and a torque of 6500 N·m were used to compare wall thickness pairs, groove combinations and changes relative to the baseline model. The baseline mass was 18.60 kg and its maximum equivalent stress was 351.75 MPa. The 13 configurations reduced mass by 4.03–14.57%. For identical groove geometry, reducing reference wall thickness from 8.5 to 8 mm decreased mass by 0.77 kg in each pair, while increasing maximum stress by 7.69–9.99%. Configurations 08, 12 and 13 met the relative screening criteria of lower mass and no increase in maximum stress; configuration 08 was the lightest of these candidates. Its reference wall thickness, groove depth and groove width were 8, 2 and 15.56 mm, respectively. Its mass was 16.81 kg, a reduction of 9.62%, and its maximum stress was 333.85 MPa, a decrease of 5.09%. Configuration 04 achieved the largest mass reduction but increased maximum stress by 26.79%. Within the configurations compared, configuration 08 offers a balance between mass reduction and stress control and is the preferred candidate for further verification.

KEYWORDS

Triangular Grooved Drill Rod; Body Mass Reduction; Reference Wall Thickness; Groove Combination; Numerical Simulation.

1. INTRODUCTION

Pre-drainage of coal-seam gas through cross-measure boreholes is an important measure for preventing coal and gas outbursts. Boreholes drilled through rock strata into the target seam provide pathways for gas removal. After sealing and connection to the drainage system, the pressure difference drives gas out of the seam, reducing its gas content and pressure before mining. Borehole quality and the continuity of the gas-flow pathway are important to drainage performance.

Screen pipes can protect the drainage pathway in soft, fractured coal seams prone to borehole collapse [1]. Collapse, narrowing and accumulated cuttings after drill-string withdrawal can obstruct pipe insertion. Previous work delivered screen pipes to the borehole bottom through the drill string and secured them before withdrawal, reducing the effect of unsupported borehole instability on installation[1]. Such procedures require compatibility between the drilling tool and the screen-pipe delivery system, so the relevant connections and mating dimensions must be retained during subsequent modifications.

Content from this work may be used under the terms of CC BY-NC 4.0 licence (https://creativecommons.org/licenses/by-nc/4.0/).
Published by Warwick Evans Publishing.

Drill-rod mass also affects the burden of manual auxiliary operations. Workers repeatedly move and support rods during transport, connection and disconnection; reducing the mass of an individual rod can ease these tasks. For a triangular grooved body, wall thinning and changes in groove geometry can both reduce material usage, but they also change the load-bearing section. Mass reduction must therefore be considered together with the resulting stress changes.

Chinese researchers have studied drill-rod cross-sections, groove parameters and mechanical performance to address cuttings transport and load-bearing requirements in soft coal seams. Wang et al. [2] developed a three-dimensional model of a grooved rod in a borehole, examined the effects of helical groove width, depth and pitch on cuttings removal, and used field trials to identify suitable parameters under the conditions investigated.

Hou et al. [3] modified a triangular cross-section for drilling in soft coal seams susceptible to outbursts. They analysed the cuttings-removal mechanism, evaluated drilling performance in the field, and considered the space available for cuttings transport together with connection wall thickness and torsional resistance.

Peng et al. [4] investigated an integral triangular helical drill rod with discontinuous helical grooves and thickened end connections. Manufacturing and heat-treatment sequences were compared, and connection make-up and break-out tests and field drilling were used to assess the proposed structure and manufacturing approach.

Yu et al. [5] investigated fracture of a 42CrMo steel triangular helical drill-rod joint using material testing, fracture-surface examination and stress analysis. Insufficient toughness and stress concentration at the thread roots were identified as contributing to early fatigue failure, showing that structural modifications must also account for material condition and local stress.

Wang et al. [6] proposed a four-wing grooved drill rod and studied mass and drilling-resistance reduction using a resistance model, finite element analysis and field trials. They also optimised groove dimensions and wall thickness. Within their study range, maximum stress increased with groove depth and decreased with wall thickness, indicating that mass-reduction parameters should be selected with load-bearing requirements in mind.

These studies provide a basis for grooved-rod design and mass-reduction analysis, but parameters for other cross-sections and end structures cannot be transferred directly. The present research group previously obtained a patent for a high-pressure sealing drill rod for gas drainage while drilling cross-measure boreholes in outburst coal seams [7]. Further development of this rod must retain its existing connecting, locating and mating requirements. The present study therefore focuses on mass reduction in the central grooved section and on matching reference wall thickness to groove dimensions.

The material, body length, maximum outer profile and end structures were kept unchanged. Thirteen configurations, each with three helical grooves and three flat grooves, were compared in terms of mass and maximum equivalent stress. Paired wall thickness comparisons at identical groove geometry and groove-combination comparisons at fixed wall thickness were used to examine mass savings and stress changes. Configurations with lower mass and no increase in maximum stress were then screened relative to the baseline model.

2. RESEARCH OBJECT AND PARAMETER CONFIGURATIONS

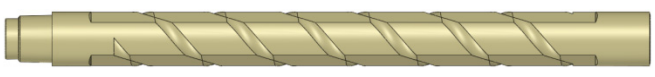

Fig 1. Model of the triangular grooved drill-rod body

The drill rod previously developed and patented by the research group [7] was used as the baseline design. The connecting, locating and mating structures at both ends were retained, while

modifications for mass reduction were confined to the central grooved section. The body consists of this central section and the two end connections, as shown in Fig. 1.

The main variables were the reference wall thickness, helical groove depth and groove width. The end structures and all other parameters outside the comparison were kept unchanged. Each configuration had three helical grooves and three flat grooves. The main dimensions of the baseline model are listed in Table 1. Its calculated mass of 18.60 kg was used as the common reference for determining the mass reduction of each configuration.

Table 1. Main geometric dimensions of the drill-rod body

Body length (mm)	Max. outer diameter (mm)	Groove width (mm)	Groove depth (mm)	Reference wall thickness (mm)
1000	89	22.7	3.5	10

2.1. Parameter Definitions and Configuration Design

The reference wall thickness, t, is the thickness at an ungrooved position in the central section. The depth and width of the helical grooves are denoted by h and b, respectively, and the flat grooves have the same depth, h. The remaining wall thickness beneath a groove also depends on its actual profile and position and is therefore distinct from the reference wall thickness. Dimensional changes were confined to the central grooved section; the body length, maximum outer diameter and end structures were unchanged.

Thirteen configurations were compared and numbered 01–13 in the order of the original data records. The reference wall thicknesses were 8, 8.5 and 10 mm, the groove depths ranged from 2 to 5 mm, and the groove widths ranged from 15.56 to 24.8 mm. The specific dimensions are listed in Table 3. The 8 and 8.5 mm wall thickness groups each contained five corresponding groove configurations. Within each wall thickness group, the helical groove depth, groove width and flat groove depth varied together in prescribed combinations.

3. LOADING CONDITIONS AND COMPARISON METHODS

3.1. Loads and Scope of the Data

The body material was S135 steel. The comparison loads were based on the output specifications of the ZDY6500LP fully hydraulic crawler drilling rig for underground use. A previous study reported a maximum pullback force of 190 kN and a rated torque range of 1750–6500 N·m for this rig Figure 2 shows the rig as presented by the manufacturer.



Fig 2. ZDY6500LP fully hydraulic crawler drilling rig

A combined axial tensile force of 190 kN and torque of 6500 N·m was used as the common loading condition, as listed in Table 2. The pullback force was treated as a tensile force along the body axis. This combination defines the loading condition for the present comparison and does not represent the complete loading history during field operation.

Table 2. Material grade and loads used for comparison

Material grade	Axial force F (kN)	Torque T (N·m)
S135	190	6500

The analysis used the ANSYS equivalent stress contour of the baseline model and the recorded results for the 13 configurations. Both the baseline model and the compared configurations corresponded to the combined loading condition of 190 kN axial tension and 6500 N·m torque. The baseline mass was 18.60 kg, and its maximum equivalent stress was 351.75 MPa. The 13 configurations had the same groove arrangement. Results for other groove arrangements or loading conditions were excluded from this comparison.

3.2. Evaluation Metrics and Comparison Methods

Body mass and maximum equivalent (von Mises) stress were used as the evaluation metrics. Mass indicates material usage and the handling burden of an individual rod, while maximum equivalent stress, hereafter referred to as maximum stress, was used to compare stress levels under combined tension and torsion. For corresponding configurations, the percentage mass reduction was calculated using Eq. (1):

$$\eta = \frac{m_{ref} - m_i}{m_{ref}} \times 100\% \tag{1}$$

where η is the percentage mass reduction, m_{ref} is the mass of the reference configuration, and m_i is the mass of the configuration being compared.

For mass reduction relative to the baseline model, the reference mass in Eq. (1) was 18.60 kg. For the wall thickness pairs, the 8.5 mm configuration served as the reference. Comparisons within a groove configuration group used the relevant dimensional combination as the reference. Mass reduction relative to the baseline model was therefore distinguished from mass reduction within each comparison group.

Two types of comparison were conducted. The first comprised five matched pairs with identical groove dimensions and reference wall thicknesses of 8 and 8.5 mm, allowing the changes associated with a 0.5 mm reduction in wall thickness to be evaluated. The second compared groove combinations at a fixed reference wall thickness. The 10 mm wall thickness group covered a different range of groove dimensions and was discussed separately.

The percentage change in maximum stress was calculated using Eq. (2). Positive values indicate an increase in stress, and negative values indicate a decrease:

$$\delta = \frac{\sigma_i - \sigma_{ref}}{\sigma_{ref}} \times 100\% \tag{2}$$

where δ is the percentage change in maximum stress, and σ_{ref} and σ_i are the maximum stresses of the reference configuration and the configuration being compared, respectively. For comparisons with the baseline model, σ_{ref} was 351.75 MPa. Comparisons of wall thickness pairs and groove combinations used their respective reference configurations. Percentage changes were rounded to two decimal places.

Groove combinations were displayed using categorical scatter plots, with both h and b shown on the horizontal axis; the flat groove depth varied together with h. These data were not interpreted as the

effect of changing groove depth or width alone. A separate mass–stress scatter plot was used to compare all complete parameter configurations.

3.3. Candidate Selection

To reduce mass without increasing the baseline maximum stress, configurations were screened using a mass below 18.60 kg and a maximum equivalent stress no greater than 351.75 MPa. Among the configurations meeting these relative criteria, preference was given to lower mass, with the groove dimensions and wall thickness considered together. The value of 351.75 MPa is only the baseline stress reference, not the allowable material stress; this screening does not replace strength verification.

4. RESULTS AND COMPARISON OF CONFIGURATIONS

4.1. Stress Distribution in the Baseline Model

Figure 3 shows the equivalent stress distribution in the baseline model under a combined axial tensile load of 190 kN and torque of 6500 N·m. The maximum equivalent stress is 351.75 MPa. This value and the calculated baseline mass of 18.60 kg are used to compare the mass reduction and stress changes of the other configurations.

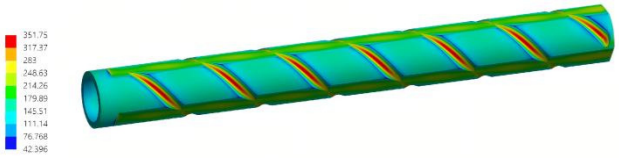

Fig 3. Equivalent stress distribution in the baseline model (MPa)

The contour plot shows pronounced stress variations near the helical grooves, with local bands of higher stress along the groove edges and relatively lower stress in the central areas of the rod faces. Groove modifications therefore require consideration of both material removal and the resulting local stress changes; overall mass alone is insufficient to assess a configuration. The exact location of the peak stress would need to be established from the original nodal results.

Table 3. Dimensions, mass, maximum equivalent stress, and mass reduction of the compared configurations

ID	*t* (mm)	*h* (mm)	*b* (mm)	Mass (kg)	Max. stress (MPa)	Mass reduction (%)
01	10	4	22.1	17.85	408.34	4.03
02	10	4.5	23.5	17.29	462.62	7.04
03	10	5	24.8	16.71	528.41	10.16
04	8	3	19.1	15.89	445.97	14.57
05	8	2.75	18.3	16.13	413.69	13.28
06	8	2.5	17.4	16.37	384.72	11.99
07	8	2.25	16.5	16.59	358.20	10.81
08	8	2	15.56	16.81	333.85	9.62
09	8.5	3	19.1	16.66	405.46	10.43
10	8.5	2.75	18.3	16.90	378.68	9.14
11	8.5	2.5	17.4	17.14	353.69	7.85
12	8.5	2.25	16.5	17.36	331.07	6.67
13	8.5	2	15.56	17.58	310.01	5.48

Table 3 lists the dimensions, mass, maximum equivalent stress, and mass reduction relative to the baseline model for all 13 configurations. Under the combined loading specified in Table 2, the mass ranges from 15.89 to 17.85 kg, and the maximum equivalent stress ranges from 310.01 to 528.41 MPa. Relative to the 18.60 kg baseline model, the mass decreases by 0.75–2.71 kg, corresponding to a reduction of 4.03–14.57%. The following sections examine paired wall-thickness changes, groove combinations, and the selection of candidate configurations.

4.2. Wall Thickness Effects on Mass and Stress

Five pairs of configurations have the same groove depth, groove width, and groove arrangement, but different reference wall thicknesses. Reducing the reference wall thickness from 8.5 to 8 mm decreases the recorded mass by 0.77 kg in every pair, corresponding to a reduction of 4.38–4.62%, while increasing the maximum equivalent stress by 7.69–9.99% (Table 4). Thus, the same reduction in wall thickness gives similar mass savings but different stress increases.

Table 4. Paired comparison for a reduction in reference wall thickness from 8.5 to 8 mm

Groove depth h (mm)	Groove width b (mm)	Mass reduction (%)	Max. stress increase (%)
3	19.1	4.62	9.99
2.75	18.3	4.56	9.25
2.5	17.4	4.49	8.77
2.25	16.5	4.44	8.19
2	15.56	4.38	7.69

As the paired groove dimensions increase from a depth of 2 mm and width of 15.56 mm to a depth of 3 mm and width of 19.1 mm, the stress increase associated with the 0.5 mm wall-thickness reduction rises from 7.69% to 9.99%. At a groove depth of 3 mm and width of 19.1 mm, for example, the maximum equivalent stress increases from 405.46 to 445.97 MPa. At a groove depth of 2 mm and width of 15.56 mm, it increases from 310.01 to 333.85 MPa. Within these paired comparisons, wall thinning produces a greater percentage stress increase for the larger groove combinations. Reference wall thickness should therefore be selected together with the groove dimensions, rather than from mass savings alone.

4.3. Effects of Groove Combinations

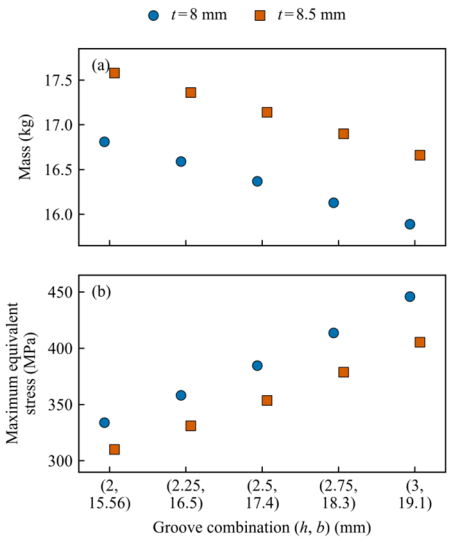

Fig 4. Comparison of body mass and maximum equivalent stress for different groove combinations

The groups with reference wall thicknesses of 8 and 8.5 mm each contain five corresponding groove combinations. Figure 4 plots mass and maximum equivalent stress against these depth–width combinations. In both groups, increasing the groove dimensions along the specified sequence reduces mass while increasing maximum equivalent stress.

At a reference wall thickness of 8 mm, changing the groove combination from h = 2 mm and b = 15.56 mm to h = 3 mm and b = 19.1 mm reduces the mass from 16.81 to 15.89 kg, a decrease of 5.47%, while increasing the maximum equivalent stress from 333.85 to 445.97 MPa, an increase of 33.58%. For the same change in groove combination at a reference wall thickness of 8.5 mm, the mass decreases from 17.58 to 16.66 kg, or by 5.23%, and the maximum equivalent stress increases from 310.01 to 405.46 MPa, or by 30.79%.

At a reference wall thickness of 10 mm, increasing the groove depth from 4 to 5 mm and the groove width from 22.1 to 24.8 mm reduces the mass from 17.85 to 16.71 kg, a decrease of 6.39%. The maximum equivalent stress increases from 408.34 to 528.41 MPa, an increase of 29.40%. These changes result from simultaneous adjustments to helical groove depth, groove width, and flat groove depth. They do not establish the independent effect of any one dimension.

All three groups show that removing more material through grooving reduces body mass but also increases stress as the remaining section changes. Groove dimensions should therefore be selected together with reference wall thickness, and each complete parameter combination should be treated as a single design configuration.

4.4. Parameter Matching and Candidate Selection

Figure 5 shows the mass and maximum equivalent stress of the 13 configurations and the baseline model. The horizontal dashed line marks the baseline maximum equivalent stress. Configuration 08 has a reference wall thickness of 8 mm, a groove depth of 2 mm, and a groove width of 15.56 mm; its mass is 16.81 kg and its maximum equivalent stress is 333.85 MPa. Configuration 11 has a reference wall thickness of 8.5 mm, a groove depth of 2.5 mm, and a groove width of 17.4 mm; its mass is 17.14 kg and its maximum equivalent stress is 353.69 MPa. Although configuration 08 has a smaller reference wall thickness, both its mass and maximum equivalent stress are lower than those of configuration 11. This comparison illustrates the importance of matching wall thickness to groove geometry.

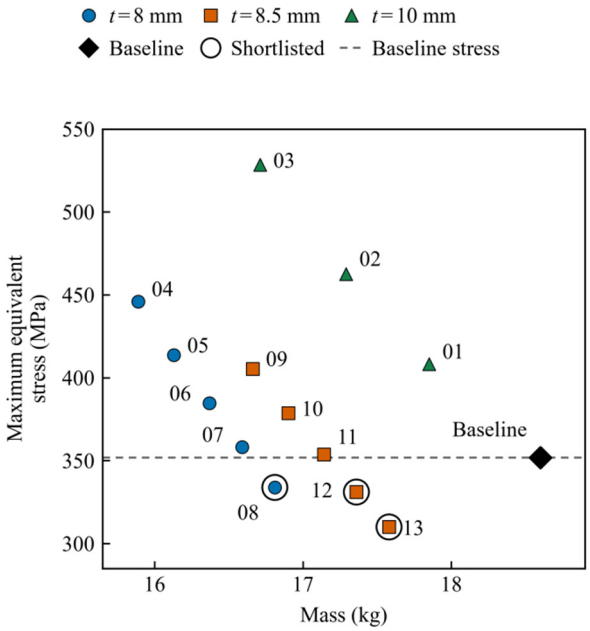

Fig 5. Mass and maximum equivalent stress of all configurations and the baseline model

Under the relative screening criteria in Section 3.3, configurations 08, 12, and 13 have both a lower mass and a maximum equivalent stress no higher than those of the baseline model. These configurations are marked by outer rings in Fig. 5. Their mass reductions are 9.62%, 6.67%, and 5.48%, respectively, and their maximum equivalent stresses decrease by 5.09%, 5.88%, and 11.87%. Table 5 compares these three candidates and the lightest configuration, 04, with the baseline model to show the trade-off between mass reduction and stress change.

Table 5. Mass and stress comparison of selected configurations with the baseline model

Config.	Mass (kg)	Mass reduction (%)	Max. stress (MPa)	Stress change (%)
Baseline	18.60	0.00	351.75	0.00
04	15.89	14.57	445.97	+26.79
08	16.81	9.62	333.85	−5.09
12	17.36	6.67	331.07	−5.88
13	17.58	5.48	310.01	−11.87

Configuration 04 has a mass of 15.89 kg, which is 2.71 kg or 14.57% below the baseline mass. However, its maximum equivalent stress rises from 351.75 to 445.97 MPa, an increase of 26.79%. Configuration 08 has a mass of 16.81 kg, a reduction of 1.79 kg or 9.62%, and a maximum equivalent stress of 333.85 MPa, a decrease of 5.09%. Compared with configuration 04, configuration 08 is 0.92 kg heavier but has a maximum equivalent stress that is 112.12 MPa lower. This comparison demonstrates the trade-off between the extent of mass reduction and the resulting stress level. As the lightest of the three candidates meeting the relative screening criteria, configuration 08 is the preferred configuration for further verification within the scope of this comparison.

4.5. Discussion and Scope of the Results

The magnitude of the differences among the candidates also warrants consideration. Configuration 12 is 0.55 kg, or 3.27%, heavier than configuration 08, while its maximum equivalent stress is only 2.78 MPa, or 0.83%, lower. Configuration 13 has the lowest maximum equivalent stress but is 0.77 kg heavier than configuration 08. If mass reduction is the main priority after the relative screening criteria have been met, configuration 08 is the preferred candidate for verification. The small stress difference between configurations 12 and 08, and the results for configurations 07 and 11 that lie slightly above the baseline value, require assessment of mesh convergence and numerical accuracy before any clear distinction in load-bearing performance can be made.

This comparison is based on the baseline stress contour plot and the retained numerical result summaries. The original ANSYS project and complete solution records were not retained, so the material inputs, detailed boundary conditions, mesh, and peak-stress locations cannot yet be checked consistently across all configurations. The available results describe differences in mass and maximum equivalent stress under the specified loading. They do not establish mesh convergence and cannot be used to assess deformation, fatigue, or field performance.

Further verification should focus on the baseline model and configuration 08, using consistent material inputs, boundary conditions, load application, and mesh settings. Stress at groove roots, groove ends, and end transitions should be examined, and load-bearing checks should use the actual material properties and operating loads. Configuration 04 can serve as a comparison with greater mass reduction to examine the stress changes associated with increased material removal by grooving.

5. CONCLUSION

(1) Across five pairs with identical groove geometry, reducing the reference wall thickness from 8.5 to 8 mm decreases the recorded mass by 0.77 kg in every pair, corresponding to a reduction of 4.38–4.62%. As the paired groove dimensions increase, the percentage increase in maximum equivalent stress rises from 7.69% to 9.99%. Similar mass savings can therefore be accompanied by different stress increases, and reference wall thickness should be selected together with groove geometry.

(2) At reference wall thicknesses of 8 and 8.5 mm, increasing the helical groove depth from 2 to 3 mm and the groove width from 15.56 to 19.1 mm, with a simultaneous increase in flat groove depth, reduces mass by 5.47% and 5.23%, respectively. Maximum equivalent stress increases by 33.58% and 30.79%, respectively. Within the combinations compared, greater mass reduction through grooving is accompanied by increased stress. Complete combinations of wall thickness and groove geometry should therefore form the basis of design selection.

(3) Relative to the baseline model, with a mass of 18.60 kg and a maximum equivalent stress of 351.75 MPa, configurations 08, 12, and 13 meet both relative screening criteria: reduced mass and no increase in maximum equivalent stress. Configuration 08 is the lightest of these candidates. Its reference wall thickness is 8 mm, groove depth is 2 mm, and groove width is 15.56 mm. Its mass of 16.81 kg represents a reduction of 9.62%, and its maximum equivalent stress of 333.85 MPa is 5.09% below the baseline value. It is therefore the preferred candidate for further verification.

REFERENCES

[1] Li, Q., Ye, S. X., & Jin, X. (2017). Application of borehole protection technique and equipment for screen pipe borehole in soft and weak seam. Coal Science and Technology, 45(6), 147–151. https://doi.org/10.13199/j.cnki.cst.2017.06.024. (in Chinese)

[2] Wang, Y. L., Zhai, X. X., & Sun, Y. N. (2011). Reasonable parameters study on grooved drill pipe used in drilling outburst coal seam. Journal of China Coal Society, 36(2), 304–307. (in Chinese)

[3] Hou, H., Ling, B. C., Luo, W., et al. (2012). Study on drilling technology with triangular drilling rod in soft and outburst seam. Coal Science and Technology, 40(8), 67–70, 74. (in Chinese)

[4] Peng, L. M., Li, G., & Pu, T. Y. (2013). Study on pilot test of integrated triangular helix drilling rod in soft and outburst seam. Coal Science and Technology, 41(8), 133–136. (in Chinese)

[5] Yu, S. J., Gong, D. M., Chen, M., et al. (2020). Cause analysis on fracture of 42CrMo steel triangular spiral drill pipe joint. Physical Testing and Chemical Analysis (Part A: Physical Testing), 56(5), 52–55. https://doi.org/10.11973/lhjy-wl202005013. (in Chinese)

[6] Wang, Y. L., Guo, J. K., Yu, Z. J., et al. (2024). Weight and resistance reduction mechanism of drilling rods for drilling in soft coal seam and its application. Coal Geology & Exploration, 52(5), 174–182. https://doi.org/10.12363/issn.1001-1986.24.01.0006. (in Chinese)

[7] Henan Polytechnic University. (2025). High-pressure sealing drill rod for gas drainage while drilling cross-measure boreholes in outburst coal seams [P]. Chinese Patent No. CN116792035B.